2011 50th IEEE Conference on Decision and Control and
European Control Conference (CDC-ECC)
Orlando, FL, USA, December 12-15, 2011

Reachability Set Subspace Computation for Nonlinear Systems using Sampling Methods

Marcus J. Holzinger
Post-Doctoral Senior Research Associate
Aerospace Engineering Department
Texas A&M University

Daniel J. Scheeres
Professor, Seebass Chair
Aerospace Engineering Sciences
University of Colorado at Boulder

***Abstract*—Computational savings in reachability set subspace computation are realized by carefully applying transversality conditions to trajectory samplings of the full reachability set. Differential constraints on the initial state and initial constraint Lagrange multiplier are developed that enforce the necessary conditions of optimality as total trajectory duration increases. Results are validated against known linear analytical results and an example is given where a 1-dimensional subspace of a 6-dimensional nonlinear problem is computed.**

I. Introduction

Computation of reachability sets has attracted significant attention over the past decades. Reachability sets have particular utility in capability and safety analyses. While the mathematical descriptions and numerical computation procedures for reachability sets for nonlinear problems are well developed, it remains that fundamentally for general, nonlinear reachability problems computation of reachability sets suffers from the curse of dimensionality.

Sometimes, however, the end user of a reachability analysis is not interested in the full reachability set, but rather a subspace thereof. This paper explores an approach in which a subspace of the reachability set may be computed while only incurring a computation penalty commensurate with the dimension of the subspace, rather than the dimension of the full reachability set.

The theory supporting formalized reachability has been extensively developed in the controls literature, and may be directly derived from optimal control theory [1], [2], [3], [4], [5]. Computing the reachability set for a given system involves satisfying the dynamic programming principle and/or solving the Hamilton Jacobi Bellman partial differential equation (HJB PDE), which has direct analogs in solving general optimal control problems. Traditional applications of reachability theory have focused on continuous differential systems, and have since been further generalized to apply to a variety of problems.

Direct analytical computation of reachable sets is difficult, and has motivated significant research aimed at determining which classes of systems may be analytically solved as well as various numerical techniques to reduce the computation burden and generate over/under-approximated reachability sets. Research into whether an analytical solution exists for a given reachability problem has demonstrated that some classes of dynamics may be analytically computed, specifically linear integrator or pure undamped oscillator systems [6]. Further, some problems have been found to be reducible to geometric problems based on insight into the propagation of the dynamics [7]. For systems with polynomial equations of motion it has been shown that reachability problems can be re-cast as a sum of squares formulation using barrier certificates and solved either directly or iteratively [8].

Over-approximations of reachable sets are desirable as they are typically performed in the context of system safety, where conservative reachability set computations are useful for risk reduction. For multi-affine systems it has been demonstrated that the state-space may be partitioned iteratively using rectangles to effeciently generate overapproximations of the reachable state-space [9]. Polytopic reachability sets, which have straightforward parameterization and computation, have been shown to provide accurate conservative outer bounds for linear and norm-bounded nonlinear systems [1], [10]. Vast improvement in over-approximated reachability set computation efficiencies has been realized for linear systems using zonotopes [11] and support functions [12]. Similar work has computed reachability sets for nonlinear systems by linearizing at each propagation step and conservatively accounting for uncertainty, also generating conservative over-approximations expressed using zonotopes [13]. Ellipsoidal reach set over- and under-approximations have been proposed for some time and have been applied to several problems [1], [14].

To reduce the dimensional complexity of the reachability set subspace computation, this paper demon-

978-1-61284-799-3/11/$26.00 ©2011 IEEE

strates that careful application of the transversality conditions on sampled individual trajectories allows reachability set subspace computation with significantly lower dimensionality-driven costs. The approach is shown to be valid for specific types of initial value functions and continuous nonlinear systems.

The contributions of this paper are a) derivation of solution dynamics along the constraint surface defined by the necessary conditions of optimality, b) a short discussion on admissible initial sets and dynamics, c) a validation of the approach by comparing solutions against known results for double-integrators with ellipsoidal initial sets, and d) an example demonstrating the successful computation of a 1-dimensional reachability set subspace with 6-dimensional nonlinear state space dynamics.

The Theory section (§II) describes the optimal control problem under consideration, applies the transversality conditions, and derives the equations of motion along the constraint surface defined by the necessary conditions of optimality. Further constraints on initial conditions are developed and it is shown that a discrete sampling of the reachability set subspace can be used to represent the reachability set subspace at future times. Examples are given in §III and conclusions / future work are discussed in §IV.

II. Theory

To properly cover the preliminaries necessary for this paper a definition of general Optimal Control Problems (OCPs) is first given, followed by a short definition of minimum time reachable sets.

Definition II.1. ***General Bolza OCP***
A general Bolza OCP may be written as

$$\begin{aligned} \underset{\boldsymbol{u}\in U}{opt}\left[\int_{t_0}^{t_f}\mathcal{L}(\boldsymbol{x}(\tau),\boldsymbol{u}(\tau),\tau)d\tau + V(\boldsymbol{x}_f,t_f)\right] \\ \dot{\boldsymbol{x}} = \boldsymbol{f}(\boldsymbol{x},\boldsymbol{u},t) \\ \boldsymbol{h}(\boldsymbol{x},t) \le \boldsymbol{0} \\ \boldsymbol{g}(\boldsymbol{x}_0,t_0,\boldsymbol{x}_f,t_f) = \boldsymbol{0} \end{aligned} \tag{1}$$

where $\boldsymbol{x} \in \mathbb{R}^n$ is the state, $\boldsymbol{u} \in \mathbb{R}^m$ is the control input, $t \in [t_0, t_f]$ is time, $\mathcal{L} : \mathbb{R}^n \times \mathbb{R}^m \times \mathbb{R} \to \mathbb{R}$ is the trajectory Lagrangian, $V : \mathbb{R}^n \times \mathbb{R} \to \mathbb{R}$ is the terminal performance function, $\boldsymbol{f} : \mathbb{R}^n \times \mathbb{R}^m \times \mathbb{R} \to \mathbb{R}^m$ captures the system differential constraints, $\boldsymbol{h} : \mathbb{R}^n \times \mathbb{R} \to \mathbb{R}^q$ defines trajectory inequality constraints, $g : \mathbb{R}^n \times \mathbb{R} \times \mathbb{R}^n \times \mathbb{R} \to \mathbb{R}^v$ expresses boundary conditions, and $U \subseteq \mathbb{R}^m$ defines the set of feasible controls.

Definition II.2. ***Minimum Time Reachability Set***
An optimal minimum time reachability set is defined as

$$\begin{aligned} &\mathcal{R}(t_f; U, \boldsymbol{f}, \boldsymbol{h}, \boldsymbol{g}, t_0) \\ &\equiv \{\boldsymbol{x}_f \mid \boldsymbol{x}_f \text{ is reachable at } t = t_f \text{ given } U, \boldsymbol{f}, \boldsymbol{h}, \boldsymbol{g}, t_0\} \end{aligned} \tag{2}$$

For minimum time reachability sets, the general OCP in Definition II.1 is modified such that $\mathcal{L}(\cdot,\cdot,\cdot) = 0$ and the 'opt' argument is considered a 'sup' argument.

Often minimum time reachability sets are determined by specifying an initial condition on the value function $V(\mathbf{x}_0, t_0)$ and computing viscosity solutions of the Hamilton Jacobi Bellman (HJB) PDE. The zero-level sets at future times t_f then represent the boundary of the minimum time reachability set $\mathcal{R}$ [15], [16], [17], [18], [19].

Because this paper is concerned with computing minimum time reachability sets over subspaces $\mathbb{R}^s$ of the full state space $\mathbb{R}^n$ ($\mathbb{R}^s \subseteq \mathbb{R}^n$), an alternate approach must be taken. The following Lemma demonstrates the type of OCP whose solutions compose the surface of a minimum time reachability set subspace.

Lemma II.1. ***Reachability Subspace OCP Without Inequality Constraints***
Each of the final states $\boldsymbol{x}_f$ from individual trajectories that together compose the optimal reachability set are solutions to the following optimal control problem without trajectory the inequality constraint $\boldsymbol{h}(\boldsymbol{x}, t) \le 0$.

$$\begin{aligned} \sup_{\boldsymbol{u}\in U}\frac{1}{2}\boldsymbol{x}_f^T\begin{bmatrix}\boldsymbol{G}_{s\times s} & \boldsymbol{0}_{s\times r}\\ \boldsymbol{0}_{r\times s} & \boldsymbol{0}_{r\times r}\end{bmatrix}\boldsymbol{x}_f \\ \dot{\boldsymbol{x}} = \boldsymbol{f}(\boldsymbol{x},\boldsymbol{u},t) \\ g(\boldsymbol{x}_0,t_0) = 0 \end{aligned} \tag{3}$$

where $\boldsymbol{G} \in \mathbb{S}^{s\times s}$ is positive definite ($rank(\boldsymbol{G}) = s$), the subspace dimension s satisfies the inequality $1 \le s \le n$, and $g(\boldsymbol{x}_0, t_0) = V(\boldsymbol{x}_0, t_0) = 0$, where $V(\boldsymbol{x}_0, t_0)$ is an initial boundary condition defined by the problem.

Proof:
It is immediately clear that choosing $g(\boldsymbol{x}_0, t_0) = V(\boldsymbol{x}_0, t_0) = 0$ causes the initial states of optimal trajectories to lie on the surface of the initial reachability set $\mathcal{R}(t_0; U, \boldsymbol{f}, \boldsymbol{h}, \boldsymbol{g}, t_0)$. The final cost term defines the square of a distance metric over the inner-product space of $\boldsymbol{G}$ over final state arguments in the subpsace $\mathbb{R}^s$. Maximizing the final distance subject to the OCP constraints is equivalent to finding a trajectory to the final distance in minimum time.
□

It must be mentioned that the removal of trajectory inequality constraints in Lemma II.1 is due largely to the

difficulty of handling such constraints in the boundary-condition manifold approach taken in remainder of this section. The inclusion of inequality constraints to the formulation is an avenue for additional work. Also, because there exists an equivalence between trajectory/Lagrangian costs $\mathcal{L}(\cdot,\cdot,\cdot)$ and the final cost $V(\cdot,\cdot)$ in Definition II.1, the choice of $\mathbf{G}_{s\times s}$ must be carefully considered given the objective function. For minimum time problems, $\mathbf{G}_{s\times s} \to \mathbb{I}_{s\times s}$ is appropriate.

From the form of the reachability subspace discussed in Lemma II.1 it is clear that application of the transversality conditions will fully define the initial and final values of the adjoint variables in terms of the initial state $\mathbf{x}_0$. The approach in this paper examines how the optimal initial state $\mathbf{x}_0$ moves along the $n+1$ dimensional constraint surface defined by $g(\mathbf{x}_0, t_0)$ and the necessary conditions of optimality. Before applying the transversality conditions, the following Lemma and Corollary regarding dynamics along constraint surfaces are introduced.

Lemma II.2. ***Constraint Satisfaction with Varying Independent Parameters***
Given an independent parameter $s \in \mathbb{R}$, parameters $\mathbf{z}(s) \in \mathbb{R}^\zeta$, and constraint $\boldsymbol{\kappa}(\mathbf{z}(s), s) = \mathbf{0}$, $\boldsymbol{\kappa}(\mathbf{z}(s), s) \in \mathbb{R}^k$, as $\mathbf{z}(s)$ varies with s, to move along the constraint surface it is necessary that

$$\frac{\mathrm{d}\boldsymbol{\kappa}}{\mathrm{d}s} = \frac{\partial \boldsymbol{\kappa}}{\partial \mathbf{z}} \frac{\mathrm{d}\mathbf{z}(s)}{\mathrm{d}s} + \frac{\partial \boldsymbol{\kappa}}{\partial s} = \mathbf{0} \tag{4}$$

Proof:
Examining variations in the independent parameter s, a Taylor Series expansion of the constraint $\boldsymbol{\kappa}(\mathbf{z}(s))$ may be written as

$$\boldsymbol{\kappa}(\mathbf{z}(s+\delta s), s+\delta s) = \boldsymbol{\kappa}(\mathbf{z}(s), s) + \frac{\mathrm{d}\boldsymbol{\kappa}}{\mathrm{d}s}\delta s + O(\|\delta s\|^2)$$

Requiring that $\boldsymbol{\kappa}(\mathbf{z}(s+\delta s), s+\delta s) = \mathbf{0}$, ignoring $O(\|\delta s\|^2)$ and higher terms, and considering arbitrarily small variations in δs, the claim in this Lemma is obtained:

$$\frac{\mathrm{d}\boldsymbol{\kappa}}{\mathrm{d}s} = \frac{\partial \boldsymbol{\kappa}}{\partial \mathbf{z}} \frac{\mathrm{d}\mathbf{z}(s)}{\mathrm{d}s} + \frac{\partial \boldsymbol{\kappa}}{\partial s} = \mathbf{0}$$

□

Corollary II.1. ***Parameter Dynamics on a Constraint Surface***
Given an independent parameter $s \in \mathbb{R}$, parameters $\mathbf{z}(s) \in \mathbb{R}^\zeta$, and constraint $\boldsymbol{\kappa}(\mathbf{z}(s), s) = \mathbf{0}$, if $\partial\boldsymbol{\kappa}/\partial\mathbf{z}$ is invertible, the parameter dynamics along the constraint surface $\boldsymbol{\kappa}(\mathbf{z}(s), s)$ as s changes are described by

$$\frac{\mathrm{d}\mathbf{z}(s)}{\mathrm{d}s} = -\left[\frac{\partial \boldsymbol{\kappa}}{\partial \mathbf{z}}\right]^{-1}\left(\frac{\partial \boldsymbol{\kappa}}{\partial s}\right) \tag{5}$$

Proof:
This result is found by solving directly for $\mathrm{d}\mathbf{z}(s)/\mathrm{d}s$ in (4).
□.

The transversality constraints are now applied to determine how a given optimal $\mathbf{x}_0$ progresses along the necessary condition constraint surfaces as time increases. After the dynamics of $\mathbf{x}_0$ are determined, a further corollary is given discussing how the reachability set subspace may be sampled and propagated as individual trajectories. Transversality conditions and dynamics along optimal trajectories are discussed in detail in many reference texts and papers [21], [22], [20].

Applying the transversality conditions to the subspace OCP defined in Lemma II.1 the following boundary conditions on the adjoints of a given optimal trajectory are written as

$$\mathbf{p}_0 = -\frac{\partial V_s}{\partial \mathbf{x}_0} - \lambda\frac{\partial g}{\partial \mathbf{x}_0} = -\lambda Dg(\mathbf{x}_0) \tag{6}$$

and

$$\mathbf{p}_f = \frac{\partial V_s}{\partial \mathbf{x}_f} + \lambda\frac{\partial g}{\partial \mathbf{x}_f} = \begin{bmatrix} \mathbf{G}\mathbf{x}_{s,f} \\ \mathbf{0}_{r\times 1} \end{bmatrix} \tag{7}$$

where $Dg(\mathbf{x}_0)$ is the differentiation operator with respect to $\mathbf{x}_0$ and $\lambda \in \mathbb{R}$ is the Lagrange multiplier associated with the initial condition constraint $g(\mathbf{x}_0, t_0)$. As the final time $t_f = t_0 + T$ is chosen, specific values of $\mathbf{x}_0(T)$ and $\lambda(T)$ can be found that maximize $V_s(\mathbf{x}_{s,f}, t_0+T) = (1/2)\mathbf{x}_s(t_0+T)^T\mathbf{G}\mathbf{x}_s(t_0+T)$. The values of $\mathbf{x}(t_0+T)$ and $\mathbf{p}(t_0+T)$ are functions of the initial time, state, and adjoints given a trajectory duration T:

$$\mathbf{x}_f(T) = \mathbf{x}(t_0+T) = \boldsymbol{\phi}_x(t_0+T; \mathbf{x}_0(T), \mathbf{p}_0(T), t_0) \tag{8}$$

$$\mathbf{p}_f(T) = \mathbf{p}(t_0+T) = \boldsymbol{\phi}_p(t_0+T; \mathbf{x}_0(T), \mathbf{p}_0(T), t_0) \tag{9}$$

To apply results from Lemma II.2 and Corollary II.1 the transversality conditions, optimal trajectory dynamics, and initial condition constraint are now formulated as $n+1$ equality constraints. If the initial time t_0 is arbitrarily allowed to be $t_0 = 0$ and it is required that $\mathbf{x}_0(T)$ and $\lambda(T)$ satisfy the initial condition constraint $g(\mathbf{x}_0(T), t_0)$, the transversality constraints (6) and (7), and the state and adjoint dynamics (8) and (9), then the following $n+1$ constraints may be constructed

$$\boldsymbol{\kappa}(\mathbf{x}_0(T), \lambda(T)) = \begin{bmatrix} \boldsymbol{\kappa}_1(\mathbf{x}_0(T), \lambda(T))_{n\times 1} \\ \kappa_2(\mathbf{x}_0(T))_{1\times 1} \end{bmatrix} = \mathbf{0} \tag{10}$$

where the following definitions are made

$$\boldsymbol{\kappa}_1(\mathbf{x}_0(T),\lambda(T)) = \begin{bmatrix} \mathbf{G} & \mathbf{0} \\ \mathbf{0} & \mathbf{0} \end{bmatrix} \boldsymbol{\phi}_x(T;\mathbf{x}_0(T),-\lambda(T)Dg(\mathbf{x}_0(T)),0) - \boldsymbol{\phi}_p(T;\mathbf{x}_0(T),-\lambda(T)Dg(\mathbf{x}_0(T)),0) \quad (11)$$

$$\kappa_2(\mathbf{x}_0(T)) = g(\mathbf{x}_0(T),0) \quad (12)$$

Consequently, for a given trajectory duration T, initial boundary condition $\mathbf{x}_0(T)$, and initial condition Lagrange multiplier $\lambda(T)$, the corresponding trajectory is a trajectory that optimizes (3) in the subspace of interest if and only if $\boldsymbol{\kappa}(\mathbf{x}_0(T),\lambda(T)) = \mathbf{0}$. This fact will be leveraged in the following sections to derive differential equations and initial condtions for $\mathbf{x}_0(T)$ and $\lambda(T)$.

Lemma II.2 motivates taking the total derivatives of each constraint with respect to the trajectory duration T. Beginning with the fist constraint generates

$$\frac{\mathrm{d}}{\mathrm{d}T}\boldsymbol{\kappa}_1(\mathbf{x}_0(T),\lambda(T)) = \begin{bmatrix} \mathbf{G} & \mathbf{0} \\ \mathbf{0} & \mathbf{0} \end{bmatrix} \left(\frac{\partial \boldsymbol{\phi}_x}{\partial T} + \frac{\partial \boldsymbol{\phi}_x}{\partial \mathbf{x}_0}\frac{\mathrm{d}\mathbf{x}_0}{\mathrm{d}T} + \frac{\partial \boldsymbol{\phi}_x}{\partial \mathbf{p}_0}\left(Dg(\mathbf{x}(T))\frac{\mathrm{d}\lambda}{\mathrm{d}T} - \lambda(T)D^2g(\mathbf{x}_0(T))\frac{\mathrm{d}\mathbf{x}_0}{\mathrm{d}T}\right)\right) - \left(\frac{\partial \boldsymbol{\phi}_p}{\partial T} + \frac{\partial \boldsymbol{\phi}_p}{\partial \mathbf{x}_0}\frac{\mathrm{d}\mathbf{x}_0}{\mathrm{d}T} + \frac{\partial \boldsymbol{\phi}_p}{\partial \mathbf{p}_0}\left(Dg(\mathbf{x}(T))\frac{\mathrm{d}\lambda}{\mathrm{d}T} - \lambda(T)D^2g(\mathbf{x}_0(T))\frac{\mathrm{d}\mathbf{x}_0}{\mathrm{d}T}\right)\right)$$

The second constraint produces

$$\frac{\mathrm{d}}{\mathrm{d}T}\kappa_2(\mathbf{x}_0(T)) = Dg(\mathbf{x}(T))\frac{\mathrm{d}\mathbf{x}_0}{\mathrm{d}T}$$

Where $D^2g(\mathbf{x}_0(T))$ is shorthand notation for $\partial^2 g(\mathbf{x}_0(T))/\partial \mathbf{x}_0^2$. Re-writing these equations and observing that $\partial\boldsymbol{\phi}_x/\partial T = d\mathbf{x}/dT$, $\partial\boldsymbol{\phi}_p/\partial T = d\mathbf{p}/dT$, $\partial\boldsymbol{\phi}_x/\partial\mathbf{x}_0 = \boldsymbol{\Phi}_{xx}(T,0)$, $\partial\boldsymbol{\phi}_x/\partial\mathbf{p}_0 = \boldsymbol{\Phi}_{xp}(T,0)$, $\partial\boldsymbol{\phi}_p/\partial\mathbf{x}_0 = \boldsymbol{\Phi}_{px}(T,0)$, and $\partial\boldsymbol{\phi}_p/\partial\mathbf{p}_0 = \boldsymbol{\Phi}_{pp}(T,0)$ where

$$\begin{bmatrix} \delta\mathbf{x}_f(T) \\ \delta\mathbf{p}_f(T) \end{bmatrix} = \begin{bmatrix} \boldsymbol{\Phi}_{xx}(T,0) & \boldsymbol{\Phi}_{xp}(T,0) \\ \boldsymbol{\Phi}_{px}(T,0) & \boldsymbol{\Phi}_{pp}(T,0) \end{bmatrix} \begin{bmatrix} \delta\mathbf{x}_0(T) \\ \delta\mathbf{p}_0(T) \end{bmatrix}$$

These substitutions produce

$$\begin{bmatrix} \frac{\partial\boldsymbol{\kappa}_1}{\partial\mathbf{x}_0} & \frac{\partial\boldsymbol{\kappa}_1}{\partial\lambda} \\ \frac{\partial\kappa_2}{\partial\mathbf{x}_0} & 0 \end{bmatrix} \begin{bmatrix} \frac{\mathrm{d}\mathbf{x}_0}{\mathrm{d}T} \\ \frac{\mathrm{d}\lambda}{\mathrm{d}T} \end{bmatrix} = \begin{bmatrix} \begin{bmatrix} \mathbf{G} & \mathbf{0} \\ \mathbf{0} & \mathbf{0} \end{bmatrix} \dot{\mathbf{x}} - \dot{\mathbf{p}} \\ 0 \end{bmatrix} \quad (13)$$

where

$$\frac{\partial\boldsymbol{\kappa}_1}{\partial\mathbf{x}_0} = \begin{bmatrix} \mathbf{G} & \mathbf{0} \\ \mathbf{0} & \mathbf{0} \end{bmatrix} \left(\boldsymbol{\Phi}_{xx}(T,0) - \lambda(T)\boldsymbol{\Phi}_{xp}(T,0)D^2g(\mathbf{x}_0(T))\right) - \left(\boldsymbol{\Phi}_{px}(T,0) - \lambda(T)\boldsymbol{\Phi}_{pp}(T,0)D^2g(\mathbf{x}_0(T))\right)$$

$$\frac{\partial\boldsymbol{\kappa}_1}{\partial\lambda} = \boldsymbol{\Phi}_{pp}(T,0)Dg(\mathbf{x}_0(T)) - \begin{bmatrix} \mathbf{G} & \mathbf{0} \\ \mathbf{0} & \mathbf{0} \end{bmatrix} \boldsymbol{\Phi}_{xp}(T,0)Dg(\mathbf{x}_0(T))$$

$$\frac{\partial\kappa_2}{\partial\mathbf{x}_0} = Dg(\mathbf{x}_0(T))$$

and

$$\frac{\partial\kappa_2}{\partial\lambda} = 0$$

As shown in Corollary II.1, because (13) is in a linear equation of the form $\mathbf{My} = \mathbf{b}$ where

$$\mathbf{M} = \frac{\partial\boldsymbol{\kappa}}{\partial\mathbf{z}} = \begin{bmatrix} \frac{\partial\boldsymbol{\kappa}_1}{\partial\mathbf{x}_0} & \frac{\partial\boldsymbol{\kappa}_1}{\partial\lambda} \\ \frac{\partial\kappa_2}{\partial\mathbf{x}_0} & 0 \end{bmatrix}$$

and

$$\mathbf{b} = -\frac{\partial\boldsymbol{\kappa}}{\partial T} = \begin{bmatrix} \begin{bmatrix} \mathbf{G} & \mathbf{0} \\ \mathbf{0} & \mathbf{0} \end{bmatrix} \dot{\mathbf{x}} - \dot{\mathbf{p}} \\ 0 \end{bmatrix}$$

with respect to $\mathrm{d}\mathbf{x}_0/\mathrm{d}T$ and $\mathrm{d}\lambda/\mathrm{d}T$, if the $n+1\times n+1$ matrix $\mathbf{M}$ is invertible, then there is a unique first order differential equation that represents the motion of $\mathbf{x}_0(T)$ and $\lambda(T)$ along the optimal trajectory constraint surface:

$$\begin{bmatrix} \frac{\mathrm{d}\mathbf{x}_0}{\mathrm{d}T} \\ \frac{\mathrm{d}\lambda}{\mathrm{d}T} \end{bmatrix} = \begin{bmatrix} \frac{\partial\boldsymbol{\kappa}_1}{\partial\mathbf{x}_0} & \frac{\partial\boldsymbol{\kappa}_1}{\partial\lambda} \\ \frac{\partial\kappa_2}{\partial\mathbf{x}_0} & 0 \end{bmatrix}^{-1} \begin{bmatrix} \begin{bmatrix} \mathbf{G} & \mathbf{0} \\ \mathbf{0} & \mathbf{0} \end{bmatrix} \dot{\mathbf{x}} - \dot{\mathbf{p}} \\ 0 \end{bmatrix} \quad (14)$$

Because $\boldsymbol{\Phi}_{xx}(T,0)$ and $\boldsymbol{\Phi}_{pp}(T,0)$ are always full rank, if $D^2g(\mathbf{x}_0(T))$ is definite, and if $\lambda(T) \neq 0$ then it is suspected that $\mathbf{M}^{-1}$ exists. However in general, depending on the scaling of the coordinates, as T increases the numerical condition number of $\mathbf{M}$ may increase arbitrarily, decreasing the accuracy of he approach. The differential equation describing the motion of $\mathbf{x}_0(T)$ and $\lambda(T)$ is written in shorthand as

$$\frac{\mathrm{d}\mathbf{x}_0(T)}{\mathrm{d}T} = \boldsymbol{\chi}_0(T,\mathbf{x}_0(T),\lambda(T),g(\mathbf{x}_0(T)),\boldsymbol{\Phi}(T,0),\dot{\mathbf{x}}(T),\dot{\mathbf{p}}(T)) \quad (15)$$

and

$$\frac{\mathrm{d}\lambda(T)}{\mathrm{d}T} = \boldsymbol{\Lambda}(T,\mathbf{x}_0(T),\lambda(T),g(\mathbf{x}_0(T)),\boldsymbol{\Phi}(T,0),\dot{\mathbf{x}}(T),\dot{\mathbf{p}}(T)) \quad (16)$$

Depending on the form of $\mathbf{M}$, there may not be closed form equations for (15) and (16). Regardless, provided that $\mathbf{M}$ is numerically invertible a numerical solution can be found.

Corollary II.2. ***Initial Conditions***
The initial conditions for $\boldsymbol{x}_{s,0}(0)$, $\boldsymbol{x}_{r,0}(0)$, and $\lambda(0)$ must satisfy

$$\begin{aligned} -\lambda(0) Dg_s(\boldsymbol{x}_{s,0}(0), \boldsymbol{x}_{r,0}(0)) &= \boldsymbol{G}\boldsymbol{x}_{s,0}(0) \\ -\lambda(0) Dg_r(\boldsymbol{x}_{s,0}(0), \boldsymbol{x}_{r,0}(0)) &= \boldsymbol{0}_{r\times 1} \\ g(\boldsymbol{x}_{s,0}(0), \boldsymbol{x}_{r,0}(0)) &= 0 \end{aligned} \tag{17}$$

where $Dg_s \in \mathbb{R}^s$ is shorthand notation for $\partial g/\partial \boldsymbol{x}_s$ and $Dg_r \equiv \partial g/\partial \boldsymbol{x}_r$, $Dg_r \in \mathbb{R}^r$.
Proof:
These initial condition requirements are found by directly evaluating (11) and (12) with $T = 0$
□

Two cases must briefly be discussed. If $\lambda(0) \neq 0$, then this constraint requires that $Dg_s(\mathbf{x}_{s,0}(0), \mathbf{x}_{r,0}(0), 0)$ and $\mathbf{G}\mathbf{x}_{s,0}(0)$ must be parallel with $\lambda(0)$ as their scaling factor, and $Dg_r(\mathbf{x}_{s,0}(0), \mathbf{x}_{r,0}(0), 0) = \mathbf{0}$. The other case, if $\lambda(0) = 0$, requires that $\mathbf{x}_{s,0}(0) = 0$, while $\mathbf{x}_{r,0}(0)$ remains free (but still subject to $g(\mathbf{x}_0(0), 0)$). If $\mathbf{x}_0(0)$ is not a solution to $g(\mathbf{x}_0(0)) = 0$, then $\lambda \neq 0$.

Several remarks regarding computational details are now given, followed by a corollary detailing how the reachability set subspace of interest may be sampled.

Remark II.1. ***Computing $\boldsymbol{\Phi}(T,0)$ and $\boldsymbol{x}_f(T)$***
Computing $\boldsymbol{\chi}_0$ and $\boldsymbol{\Lambda}$ (analytically or numerically) requires $\boldsymbol{\Phi}(T,0)$ and $\boldsymbol{x}_f(T)$. While future work will examine methods to generate differential equations $\mathrm{d}\boldsymbol{\Phi}/\mathrm{d}T$ and $\mathrm{d}\boldsymbol{x}_f/\mathrm{d}T$, the quantities $\boldsymbol{\Phi}(T,0)$ and $\boldsymbol{x}_f(T)$ can be computed by implementing a nested numerical integration operation inside of the integration operation for $\mathrm{d}\boldsymbol{x}_0/\mathrm{d}T$ and $\mathrm{d}\lambda/\mathrm{d}T$. This nested integration is qualitatively similar to approaches used in solving Model Predictive Control problems, and makes computing reachability subsets over large ranges of independent parameters computationally burdensome, but does not interfere with the proof of concept demonstrated in this paper.

Remark II.2. ***Local Evaluation of the Initial Condition Constraint***
In the derivation of the optimal intial state dynamics (15) and Lagrange multiplier dynamics (16), no particular form of $g(\boldsymbol{x}_0(0), 0) = 0$ was considered. The derivation does impose that at the evaluation point $\boldsymbol{x}_0(T)$, both $Dg(\boldsymbol{x}_0(T)$ and $D^2g(\boldsymbol{x}_0(T)$ be well defined. This suggests that a piecewise definition of $g(\boldsymbol{x}_0, t_0) = 0$ may be used to define initial reachability sets.

Corollary II.3. ***Sampling a Reachability Subspace***
Given an OCP of the form shown in Lemma II.1, equation (3), the surface of the initial reachability set surface defined by $g(\boldsymbol{x}_0(0), t_0) = 0$ may be represented by computing points $\boldsymbol{x}_{s,f}(T)$ found by propagating a sampling set of initial conditions $\boldsymbol{x}_0(T)$ subject to dynamics (15) and $\lambda(T)$ subject to dynamics (16), with $\boldsymbol{x}_0(0)$ and $\lambda(0)$ satisfying Corollary II.2.
Proof:
Because $V(\boldsymbol{x}_0, t_0) = g(\boldsymbol{x}_0, t_0) = 0$, any feasible initial $\boldsymbol{x}_0$ is on the boundary of the reachability set at time t_0. Initial optimal trajectories starting from $\boldsymbol{x}_0(0)$ satisfying (15) and associated Lagrange multipliers $\lambda(0)$ satisfying (16) necessarily define the maximum reachability surface subspace as the necessary conditions are satisfied and the optimal control maximizes the final value function.
□

Remark II.3. ***Computational Effort***
Computing a reachability subspace of dimension s assuming a full state-space dimension of n and N samplings in each subspace dimension requires approximately $N^{s-1}(n+1)(n^2+n)$ computations. For each of the N^{s-1} samplings, n+1 states must be propagated, and for each integration step a nested integration of n^2+n states must be made.

Because each trajectory forming a point-wise reachability surface approximation exactly satisfies the necessary conditions of optimality (to within numerical integration tolerances), the resulting reachability subspace surface is not guaranteed to be either a over- or under-approximation. Locally, the transversality conditions may be used to construct tangent planes to the true reachability surface, defined by the tangent normal unit vector $\hat{\mathbf{p}}_f(T)$.

In general, as T is increased, a surface region in a point-wise approximation of a reachability set may experience increasing or decreasing sampling density. To efficiently sample such regions, schemes in which arbitrary distance metrics are used to identify densely or sparsely populated regions may be used. In the event that a region is deemed too sparse, additional samples may be added to the region as desired.

It remains that it must be determined how $\boldsymbol{\Phi}(T,0)$ changes as $\mathbf{x}_f(T)$, $\mathbf{x}_0(T)$, and $\lambda(T)$ move along the constraint surface. To start, the total derivative of variations in the final state and adjoint with respect to trajectory

duration T is taken

$$\frac{\mathrm{d}}{\mathrm{d}T}\begin{bmatrix}\delta\mathbf{x}(T)\\ \delta\mathbf{p}(T)\end{bmatrix} = \frac{\mathrm{d}\mathbf{\Phi}(T,0)}{\mathrm{d}T}\begin{bmatrix}\delta\mathbf{x}_0(T)\\ \delta\mathbf{p}_0(T)\end{bmatrix} + \mathbf{\Phi}(T,0)\begin{bmatrix}\frac{\mathrm{d}\delta\mathbf{x}_0(T)}{\mathrm{d}T}\\ \frac{\mathrm{d}\delta\mathbf{p}_0(T)}{\mathrm{d}T}\end{bmatrix}$$

The linearized time derivative of variations of the state and adjoint are

$$\frac{\mathrm{d}}{\mathrm{d}T}\begin{bmatrix}\delta\mathbf{x}(T)\\ \delta\mathbf{p}(T)\end{bmatrix} = \mathbf{A}(T)\begin{bmatrix}\delta\mathbf{x}(T)\\ \delta\mathbf{p}(T)\end{bmatrix}$$

Combining generates

$$\mathbf{A}(T)\mathbf{\Phi}(T,0)\begin{bmatrix}\delta\mathbf{x}_0(T)\\ \delta\mathbf{p}_0(T)\end{bmatrix} = \frac{\mathrm{d}\mathbf{\Phi}(T,0)}{\mathrm{d}T}\begin{bmatrix}\delta\mathbf{x}_0(T)\\ \delta\mathbf{p}_0(T)\end{bmatrix} + \mathbf{\Phi}(T,0)\begin{bmatrix}\frac{d\delta\mathbf{x}_0(T)}{dT}\\ \frac{d\delta\mathbf{p}_0(T)}{dT}\end{bmatrix}$$

III. Examples

A. Subset Computation Validation

To validate the approach the first example chosen is a linear double-integrator system. This system benefits from known analytical solutions for maximum reachable position given an ellipsoidal initial set. The dynamics may be written as

$$\dot{\mathbf{x}} = \begin{bmatrix}\dot{d}\\ \dot{v}\end{bmatrix} = \begin{bmatrix}0 & 1\\ 0 & 0\end{bmatrix}\begin{bmatrix}d\\ v\end{bmatrix} + \begin{bmatrix}0\\ 1\end{bmatrix}u \qquad (18)$$

where d is the distance, v is the velocity, and u is the acceleration input. The optimal control policy for minimum time is $u^* = u_m \operatorname{sgn}(p_v)$, where for this problem $u_m = 1$. The following problem parameters are used:

$$g(\mathbf{x}_0) = \mathbf{x}_0^T\mathbf{x}_0 - 1 = 0$$

$$V(\mathbf{x}_f, t_f) = \frac{1}{2}\mathbf{x}_f^T\begin{bmatrix}1 & 0\\ 0 & 0\end{bmatrix}\mathbf{x}_f \rightarrow \mathbf{G} = G = 1$$

Applying Corollary II.2, the initial state and Lagrange multiplier are then

$$\mathbf{x}_0(0)^T = \begin{bmatrix}1 & 0\end{bmatrix}^T,\ \lambda(0) = -\frac{1}{2}$$

The total trajectory duration is chosen to be $T = 1$. The differential equations for $d\mathbf{x}_0(T)/dT$ and $d\lambda(T)/dT$ are propagated using Matlab's ode45 routine with absolute and relative tolerances of $1e^{-12}$ and $1e^{-9}$, respectively. Figure 1 plots the constraint surface $g(\mathbf{x}_0(T)) = 0$, the optimal initial states $\mathbf{x}_0^*(T)$, final states $\mathbf{x}_f^*(T)$, and corresponding trajectories as a function of total trajectory duration.

Figure 2 plots only the position subspace and associated optimal trajectories as a function of total trajectory duration T. The initial position, velocity, and optimal Lagrange multiplier are plotted as a function of total trajectory duration in Figure 3. For the entire duration the constraint satisfaction residual remains below $3e^{-7}$. Comparing with known analytical results, the error in the

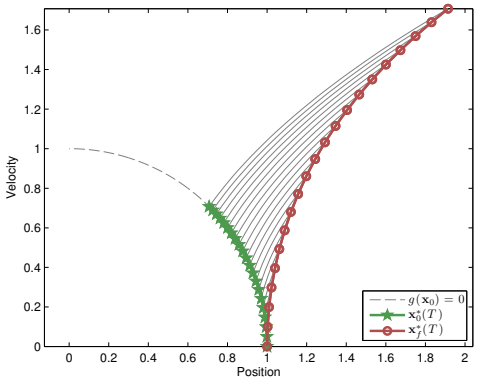

Fig. 1. Example 1: Phase Space

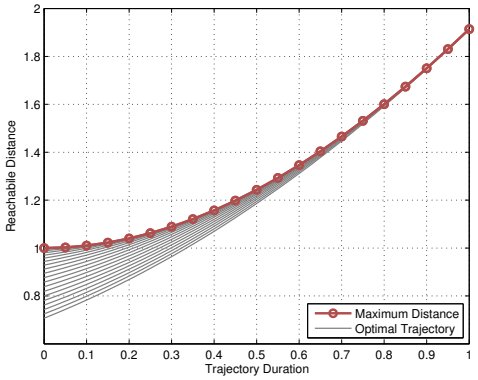

Fig. 2. Example 1: Reachable Distance

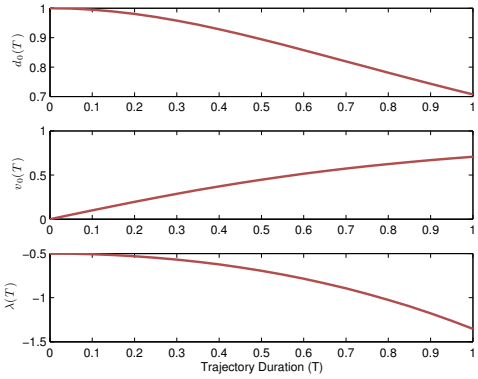

Fig. 3. Example 1: $\mathbf{x}_0(T)$ and $\lambda(T)$ Solution

final position and velocity remain on the order of $1e^{-9}$ for the entire trajectory duration. Consistent with most ode45 integration solutions, the solution accumulates integration error, causing constraint satisfaction error to increase over time. As can be seen, the approach outlined in this paper agrees nicely with analytical results for the double-integrator system.

B. Example 2: 3-DOF Coupled Duffing Oscillator

To demonstrate the utility of the subspace computation approach for higher dimensional nonlinear problems, this example examines the reachability set subspace of a 3-DOF coupled Duffing oscillator. The nonlinear equations of motion are

$$\begin{aligned} m_1\ddot{x}_1 &= -k_{1,1}x_1 - k_{1,3}x_1^3 - f_1\dot{x}_1 \\ &+k_{2,1}\left(x_2 - x_1\right) + k_{2,3}\left(x_2 - x_1\right)^3 + f_2\left(\dot{x}_2 - \dot{x}_1\right) \end{aligned} \tag{19}$$

$$\begin{aligned} m_2\ddot{x}_1 &= -k_{2,1}\left(x_2 - x_1\right) - k_{2,3}\left(x_2 - x_1\right)^3 - f_2\left(\dot{x}_2 - \dot{x}_1\right) \\ &+k_{3,1}\left(x_3 - x_2\right) + k_{3,3}\left(x_3 - x_2\right)^3 + f_3\left(\dot{x}_3 - \dot{x}_2\right) \end{aligned} \tag{20}$$

$$\begin{aligned} m_3\ddot{x}_1 &= -k_{3,1}\left(x_3 - x_2\right) - k_{3,3}\left(x_3 - x_2\right)^3 - f_3\left(\dot{x}_3 - \dot{x}_2\right) \\ &+F \end{aligned} \tag{21}$$

Here, for $i = 1, 2, 3$, m_i represent the masses, x_i represent the positions, $\dot{x}_i$ are the velocities, $k_{i,1}$ represent the linear spring coefficients, $k_{i,3}$ represent the cubic spring coefficients, f_i represent viscous friction coefficients, and F is forcing term acting only on m_3 with a maximum force of F_m. The state-space is defined as

$$\mathbf{x}^T = \begin{bmatrix} x_1 & x_2 & x_3 & \dot{x}_1 & \dot{x}_2 & \dot{x}_3 \end{bmatrix}^T$$

For this example the following parameters are chosen:

$$g(\mathbf{x}_0) = \mathbf{x}_0^T\mathbf{x}_0 - 1 = 0$$

$$V(\mathbf{x}_f, t_f) = \frac{1}{2}\mathbf{x}_f^T\left[\text{diag}\left(\begin{bmatrix} 0 & 0 & 1 & 0 & 0 & 0 \end{bmatrix}\right)\right]\mathbf{x}_f$$

$$\begin{aligned} m_1 = m_2 = m_3 = 1 \qquad & k_{1,1} = k_{2,1} = k_{3,1} = 1 \\ k_{1,3} = k_{2,3} = k_{3,3} = \tfrac{1}{9} \qquad & f_1 = f_2 = f_3 = 1 \end{aligned}$$

$$u_m = \frac{F_m}{m_3} = 1,\ t_0 = 0,\ t_f = 2\pi,\ T = 2\pi$$

$$\mathbf{x}_0(0)^T = \begin{bmatrix} 0 & 0 & 1 & 0 & 0 & 0 \end{bmatrix}^T,\ \lambda(0) = -\frac{1}{2}$$

Because this is a minimum time problem and the system dynamics are affine with control, the optimal control policy is $u^* = -u_m\,\text{sgn}(\dot{p}_3)$. The differential equations for $d\mathbf{x}_0(T)/dT$ and $d\lambda(T)/dT$ are propagated in Matlab using ode45 with absolute and relative integration tolerances of $1e^{-12}$ and $1e^{-9}$, respectively.

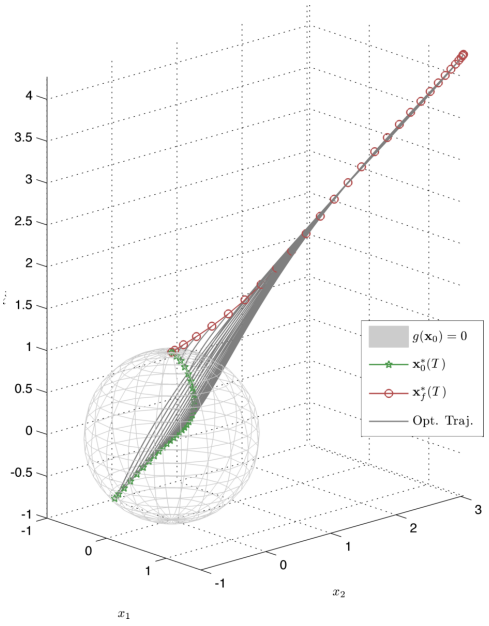

Fig. 4. Example 2: Full Position Subspace

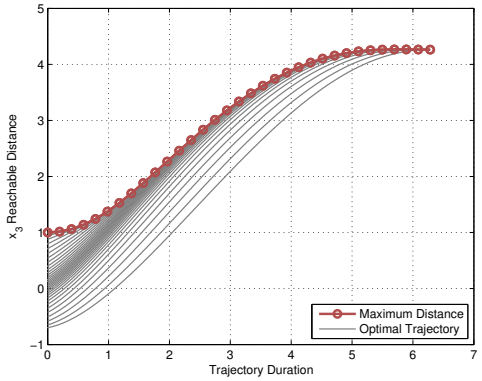

Fig. 5. Example 2: Reachable Distance

Figure 4 plots the position subspace along with position components of the optimal initial states $\mathbf{x}_0(T)$ and final states $\mathbf{x}_f(T)$. The sphere plotted is the position subspace of the hyper-sphere initial condition constraint $g(\mathbf{x}_0) = 0$. The maximum reachable distance x_3 over trajectory duration T along with corresponding optimal trajectories is plotted in Figure 5. Figure 6 plots the full optimal initial state $\mathbf{x}_0(T)$ and Lagrange multiplier $\lambda(T)$ as a function of total trajectory duration T. Note that the constraint satisfaction discrepancy remains below $1e^{-6}$ for $T = 2\pi$.

The total solution time for the results plotted in Figures 4, 5, and 6 is 1999 seconds on a MacBook Pro

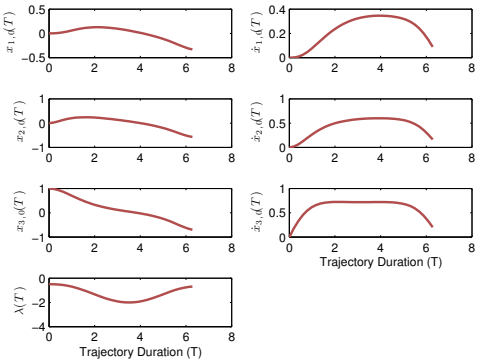

Fig. 6. Example 2: $\mathbf{x}_0(T)$ and $\lambda(T)$ Solution

2.4GHz Intel Core 2 Duo processor with 4GB 667MHz DDR2 SDRAM. The maximum constraint satisfaction residual occurred at $T = 2\pi$ and was $1.6e^{-6}$. Faster solutions may be found using relaxed absolute and relative integration tolerances. Computing the solution with absolute and relative integration tolerances of $1e^{-6}$ and $1e^{-3}$ respectively yielded results with maximum constraint satisfaction errors of 0.045 in approximately 20 seconds on a the same laptop.

IV. Conclusions and Future Work

The transversality conditions are applied to the minimum time equivalent OCP generating a set of $n + 1$ necessary conditions on the optimal initial state $\mathbf{x}_0(T)$ and Lagrange multiplier $\lambda(T)$. Dynamics for $\mathbf{x}_0(T)$ and $\lambda(T)$ are derived which move the optimal solution along the constraint surface defined by the necessary conditions of optimality. By sampling the initial reachability subspace, it is shown that the reachability subspace after a trajectory duration of T may be found by numerically integrating the constraint surface dynamics. The approach is validated for the double-integrator system, and a nonlinear 6-dimensional example is given to demonstrate the utility of the approach. Future work will focus on exploring how best to sample $g(\mathbf{x}_0, t_0) = 0$ to approximate $V(\mathbf{x}_f, t_f) = 0$, decreasing computational requirements by developing differential forms for the final state $\mathbf{x}_f(T)$ and state transition matrix $\mathbf{\Phi}(T, 0)$ dynamics.

Acknowledgments

This work is supported by AFOSR Grant No. FA9550-08-1-0460.

References

[1] P. Varaiya, "Reach set computation using optimal control," Proceedings of the KIT Workshop on Verification of Hybrid Systems, pages 377-383, Grenoble, France, 1998.

[2] A. B. Kurzhanski, P. Varaiya, "Dynamic Optimization for Reachability Problems", Journal of Optimization Theory and Applications, Vol. 108, No. 2, pp 227-251, February 2001.

[3] J. Lygeros, "On the Relation of Reachability to Minimum Cost Optimal Control," IEEE Conference on Decision and Control, pages 1910-1915, Vol. 2, Las Vegas, December 2002.

[4] J. Lygeros, "On Reachability and Minimum Cost Optimal Control," Automatica, 40(6), pages 917-927, June, 2004.

[5] A. B. Kurzhanski, I. M. Mitchell, P. Varaiya, "Optimization Techniques for State-Constraineed Control and Obstacle Problems," Journal of Optimization Theory and Applications, Volume 128, Number 3, 499-52, 2006.

[6] Lafferriere, G.; Pappas, G. J., and Yovine, S., "A new Class of decidable Hybrid Systems," Hybrid Systems: Computation and Control, Springer, pages 137-151, 1999.

[7] Schmidt, C.; Oechsle, F., and Branz, W., "Research on trajectory planning in emergency situations with multiple objects," Proc. of the IEEE Intelligent Transportation Systems Conference, pages 988-992, 2006.

[8] Prajna, S. and Jadbabaie, "A. Safety Verification of Hybrid Systems Using Barrier Certificates," Hybrid Systems: Computation and Control, Springer, pages 477-492, 2004.

[9] Kloetzer, M., and Belta, C., "Reachability Analysis of Multi-affine Systems," Hybrid Systems: Computation and Control, Springer, pages 348-362, 2006.

[10] I. Hwang, D. M. Stipanovic, and C. J. Tomlin, "Applications of Polytopic Approximations of Reachable Sets to Linear Dynamic Games and a Class of Nonlinear Systems," Proceedings of the American Control Conference, pages 4613-4619, Vol. 6, Denver, Colorado, 2003.

[11] Girard, A.; Guernic, C. L., and Maler, O., "Efficient Computation of Reachable Sets of Linear Time-Invariant Systems with Inputs," Hybrid Systems: Computation and Control, pages 257-271, Springer, 2006.

[12] Girard, A., and Guernic, C. L., "Efficient Reachability Analysis for Linear Systems using Support Functions," Proc. of the 17th IFAC World Congress, pages 8966-8971, 2008.

[13] Althoff, M.; Stursberg, O., and Buss, M., "Reachability Analysis of Nonlinear Systems with Uncertain Parameters using Conservative Linearization," Proc. of the 47th IEEE Conference on Decision and Control, pages 4042-4048, 2008.

[14] A. B. Kurzhanski, P. Varaiya, "Ellipsoidal Techniques for Reachability Analysis," Hybrid Systems: Computation and Control, pages 202-214, Springer, 2000.

[15] M. G. Crandall, L. C. Evans, and P. L. Lions, "Some properties of viscosity solutions of Hamilton-Jacobi equations," Transactions of the American Mathematical Society, Vol. 282, No. 2, pages 487-502, April 1984.

[16] S. Osher, J. Sethian, "Fronts propagating with curvature-dependent speed:Algorithms based on Hamilton-Jacobi formulations," Journal of Computational Physics, 79, pages 12-49, November 1988.

[17] J. A. Sethian, "Level set methods: Evolving interfaces in geometry, fluid mechanics, computer vision, and materials science." New York: Cambridge University Press, 1996.

[18] A. M. Bayen, C. J. Tomlin, "A construction procedure using characteristics for viscosity solutions of the Hamilton-Jacobi equation," IEEE Conference on Decision and Control, pages 1657-1662, vol. 2, Orlando, 2001.

[19] I. M. Mitchell, "A Toolbox of Level Set Methods," UBC Department of Computer Science Technical Report TR-2007-11, June 2007.

[20] W. H. Fleming, H. M. Soner, "Controlled Markov Processes and Viscosity Solutions, 2^{nd} Ed." New York, Springer, 2006

[21] D. F. Lawden, "Analytical Methods of Optimization," Mineola, NY, Dover Publications, 2003.

[22] H. J. Sussmann, "Geometry and Optimal Control," Mathematical Control Theory, Springer-Verlag, 1998, 140-198.